Antitumor Immune Mechanisms of the Anti-Complement Factor H Antibody GT103

Ryan T. Bushey[1], Ruchi Saxena[2], Michael J. Campa[1], Elizabeth B. Gottlin[1], You-Wen He[2], Edward F. Patz, Jr.[1,3*]

[1]Department of Radiology, Duke University School of Medicine, Durham, NC 27710
[2]Department of Immunology, Duke University School of Medicine, Durham, NC 27710
[3]Department of Pharmacology and Cancer Biology, Duke University School of Medicine, Durham, NC 27710

Running Title
Immune modulation by an anti-CFH antibody

Abbreviations
ADCP, antibody dependent cellular phagocytosis; CDC, complement dependent cytotoxicity; CFH, complement factor H; CR2, complement receptor 2; DAMP, damage associated molecular pattern; DC, dendritic cell; FBS, fetal bovine serum; MFI, mean fluorescence intensity; NHS, normal human serum; NSCLC, non-small cell lung cancer; scRNA-seq, single cell RNA sequencing; TMA, tissue microarray

***Corresponding Author**
Edward F. Patz, Jr., Box 3808, Duke University Medical Center, Durham, NC 27710, patz0002@mc.duke.edu

Conflicts of Interest
EFP is a Founder, Board Member, and the CEO of Grid Therapeutics, LLC. MJC and EBG are Founders of Grid Therapeutics, LLC. RTB, RS, and YWH declare no potential conflicts of interest.

Word Count: 3823 excluding Title Page, Materials and Methods, and References

Figure Count: 6

Abstract

Development of novel therapeutic antibodies that not only kill tumor cells but modulate the adaptive immune response has the potential to produce long term anti-cancer immunity and a durable clinical response. We previously reported the discovery of anti-complement factor H (CFH) autoantibodies in lung cancer patients that were associated with early stage disease and exceptional outcomes. The human monoclonal antibody GT103, produced from a single CFH autoantibody-expressing B cell of a lung cancer patient, recognizes a conformationally distinct epitope on tumor cells, kills tumor cells, and inhibits tumor growth in animal studies. Recent experiments have shown that GT103 restructures the tumor microenvironment and initiates a robust antitumoral adaptive immune response. The current study further elucidates several mechanisms by which GT103 kills tumor cells and drives the immune program. Here we show GT103 has specificity for tumor cells without binding to native soluble CFH or normal tissues. GT103 causes complement C3 split product deposition on tumor cells *in vitro* and *in vivo,* triggers antibody-dependent cellular phagocytosis, and increases translocation of the danger associated molecular pattern molecule calreticulin to the plasma membrane. We also demonstrate that GT103 causes B cell activation *in vitro* and *in vivo,* and that GT103 antitumor activity *in vivo* is B cell dependent. The complex mechanism of GT103, a tumor specific antibody that kills tumor cells and stimulates an immune response, supports further development of this human-derived antibody as a novel therapeutic option for patients with lung cancer.

Introduction

Immune checkpoint inhibitors have made a significant impact on the treatment of cancer; however, they are only effective in a minority of patients (1). A more comprehensive understanding of how to initiate and drive a robust antitumor immune response will provide valuable insight into developing novel therapeutic strategies. We suggest that for a durable clinical response, a drug must not only target and kill tumor cells, but also engage adaptive immunity. Tumors are composed of a variable mixture of tumor and host cells, and by studying the native immune responses of patients that do exceptionally well we may obtain invaluable information about mechanisms by which to create effective antitumor immunity.

Prior studies have shown that tumor rejection initiated by autoantibodies can promote an adaptive immune response (2,3). In a search for autoantibodies correlated with a more favorable cancer phenotype, we found that patients with early stage non-small cell lung cancer (NSCLC) had a significantly higher incidence of anti-complement factor H (CFH) autoantibodies than those with more advanced stage disease (4). These autoantibodies were also associated with increased time to recurrence in stage I NSCLC patients (5). CFH is a regulatory protein that protects host cells from destruction by the alternative pathway of complement-dependent cytotoxicity (CDC) but it is also hijacked by tumor cells as an evasive strategy to counter antitumor immunity (6-11). We cloned the genes encoding anti-CFH autoantibodies from single antigen-specific B cells of NSCLC patients and are developing one of them, GT103 (formerly mAb7968), as a therapy for cancer (12). GT103 recognizes an altered conformational epitope of CFH on tumor cells, kills tumor cells *in vitro* by CDC, and inhibits tumor growth and metastasis *in vivo* while having no observable effect on normal cells (12-14). More recently, Saxena et al. (15) found that GT103 promotes the formation of an antitumor microenvironment characterized by reduced populations of immunosuppressive T regulatory cells and myeloid derived suppressor

cells and increased populations of antigen-specific CD4+ and CD8+ T cells.

The purpose of the current study was to further elucidate the mechanisms by which GT103 targets and kills tumor cells. We report the following mechanistic findings: First, GT103 specifically binds to tumor tissues but not native soluble CFH or normal tissues. Second, as a result of inducing CDC of tumor cells, GT103 causes translocation of the immunogenic damage associated molecular pattern (DAMP) molecule calreticulin to the plasma membrane. Third, by virtue of binding to tumor cells in the absence of complement, GT103 directly promotes their antibody-dependent cellular phagocytosis (ADCP). Fourth, GT103-induced CDC results in the release of bioactive complement split products known to bind to receptors on B cells. Fifth, GT103 promotes B cell activation *in vitro* and *in vivo* and the antitumor growth activity of GT103 depends on B lymphocytes. The multi-pronged mechanism of GT103, combined with an extraordinary safety profile in a Phase 1b clinical trial, supports GT103 as a novel treatment for lung cancer.

Materials and Methods

Cell lines

The mouse CMT167 lung tumor cell line was a kind gift from Raphael Nemenoff (University of Colorado). The human lung tumor cells lines NCI-H460 ("H460") and A549 were obtained from American Type Culture Collection. CMT167 was tested for mycoplasma and found to be negative before use in animal experiments.

Tumor growth in mice

As described in Saxena et al. (15), six- to eight-week-old female C57BL/6 mice were implanted s.c. in the right flank with 2.0×10^5 CMT167 lung tumor cells. One week after inoculation, mice were treated for 2 weeks with murine GT103 (mGT103 - 200 µg/mouse i.p.) or

a control solution (murine IgG2a [mIgG2] - 200 µg/mouse i.p.) three times weekly. Murine GT103 has the identical complementarity determining region as human GT103, and the autoantibody from which human GT103 was derived, set in a murine IgG2a framework (12).

For the B cell ablation experiment, mice were injected with anti-CD20 (Biolegend, Inc. Cat# 152104, RRID:AB_2629619 - 250 µg/mouse i.v.) three days prior to tumor inoculation. B cell-depleted and nondepleted mice were inoculated s.c. with 2.5 x 10^5 CMT167 cells. Five days after tumor cell inoculation, when tumors were palpable, mice in each group were randomized and dosed three times a week with either control mIgG2 (100 µg i.p.) or mGT103 (200 µg i.p.). Bidimensional tumor measurements were made every other day and tumor volume was calculated using the formula V = (smallest diameter)^2 x the largest diameter / 2. After the mice were sacrificed, tumors were excised and a portion of the excised tumors was used to prepare single cell suspensions for flow cytometry in order to verify B cell depletion, as described below. Tumor volume was plotted as mean ± SEM for each treatment group. For all animal experiments, mice were euthanized according to protocols approved by the Duke University Institutional Animal Care and Use Committee.

Preparation of single cell suspensions and flow cytometry

Single cell suspensions from tumor tissue were prepared and analyzed for different immune cell populations by flow cytometry. Briefly, the tissues were minced into small pieces using scissors and incubated with 200U/ml collagenase (Thermo Fisher Scientific) and 100U/ml DNase I (Sigma Aldrich) in RPMI for 30 min at 37°C. Single cell suspensions were stained with fluorescently-conjugated antibodies against CD19 (Biolegend Cat# 115520, RRID:AB_313655) and CD45 (Biolegend Cat# 103116, RRID:AB_312981) to validate B cell depletion in mice

injected with anti-CD20 antibody. Flow cytometric analysis was performed on a FACSCanto flow cytometer (BD Biosciences) and the results were analyzed using FlowJo software.

Single cell RNA sequencing (scRNA-seq)

We performed scRNA-seq analysis, comparing gene transcription in CMT167 tumors of mGT103- and mIgG2a control-treated tumor-bearing mice as described previously in detail (15). In brief, tumors were initiated as above, treatment commenced when tumors were palpable, and after two weeks of treatment, mice were sacrificed, tumors excised, and single cell suspensions of tumor tissue were prepared from the pooled tumor tissue from 3 mice in each in each group. CD45+ cells were isolated, single cells were encapsulated and subjected to reverse transcription, and sequencing libraries were prepared and sequenced. Sequences were subjected to standard QC, filtering, normalization, sample integration and clustering steps, and analysis of differential gene expression between the two groups was performed as described.

Immunofluorescence staining of frozen mouse tissues with GT103

Mouse tumor, lung, and kidney specimens used in this study were from the vehicle-treated arm of a CMT167 tumor growth study. After the mice were sacrificed, tumors or organs were frozen, after which they were cut into 7 µm sections and placed on slides for immunofluorescence analyses. For staining with GT103, sections were fixed in 4% paraformaldehyde for 20 min at room temperature and blocked in 5% goat serum (Sigma Cat# G9023)/PBS (Thermo Fisher Cat# 10010-023) with 0.5% Tween (PBST) for 1 hr at room temperature. The samples were incubated with human GT103, or a subtype-matched IgG3 control antibody (Dendritics Cat# DDXCHO3P), at 5 or 50 µg/ml overnight at 4°C in 1% goat serum/PBST, followed by an Alexa Fluor 488 goat anti-human secondary antibody (Invitrogen Cat# A11013) at 10 µg/ml in 1% goat serum/PBST for 2 hrs at room temperature. Slides were

washed 4x with PBST following the primary and secondary antibody incubations. Hoechst DNA stain (Thermo Fisher Cat# 62249) was used at 1 μg/ml for 5 mins at room temperature. Prolong Gold (Thermo Fisher Cat# P10144) was used as the mountant. Sections were stained with secondary antibody alone as a negative control. All microscopy was performed using a Zeiss Axio Imager Widefield Fluorescent Microscope in the Duke Light Microscopy Core Facility.

Immunofluorescence staining of human lung tumor and normal human lung with GT103

The use of human specimens in this study was approved by the Duke Health Institutional Review Board. Formalin-fixed paraffin-embedded normal lung and human lung tumor tissue from a tissue microarray (TMA) were cut into 7 μm sections and placed on slides. The TMA had 33 usable lung tumor spots from individuals with NSCLC. Anti-CFH autoantibody status was determined by serum ELISA as previously described (5). Samples were rehydrated using a xylene and ethanol gradient, and antigen retrieval was performed using a citrate buffer (Sigma Cat# C9999) and heating in a microwave oven. Blocking was done in 5% goat serum/PBST for 1 hr at room temperature. Murinized (IgG2a) GT103 was used at 50 μg/ml in 1% goat serum/PBST overnight at 4°C. A negative control murine IgG2a antibody (Bio X Cell Cat# BP0085) was used at the same concentration. An Alexa Fluor 488 goat anti-mouse secondary antibody (Invitrogen Cat# A11001) was used at 10 μg/ml in 1% goat serum/PBST for 2 hrs at room temperature. Washes after primary and secondary antibody incubations, DNA staining, mounting, and imaging were performed as described above. For fluorescence quantitation, images were captured for each of 2 spots and the mean fluorescence intensity (MFI) of GT103 staining was divided by the MFI of DNA stain for each spot to account for differences in the number of cells in each image.

Competition ELISA

We have previously determined the epitope to which GT103 binds (13). A biotinylated GT103 epitope-containing peptide (GPPPPIDNGDITSFPGGG-K(biotin); epitope underlined), at 2 μg/ml in Ca^{++}- and Mg^{++}-free Dulbecco's phosphate-buffered saline (DPBS, Thermo Fisher Cat# 14190-144), was immobilized in the wells of an ELISA plate precoated with NeutrAvidin (Thermo Fisher Cat# PI31000) by overnight incubation at 4°C. The wells of the plate were then washed 4 times with PBST and incubated at room temperature for 90 min with GT103 (0.25 to 0.0039 μg/ml in 2-fold dilutions) either alone or previously incubated with 50 μg/ml CFH (Complement Technology, Inc., Tyler, TX, Cat# A137) for 0 or 1 h at room temperature, or 24 h at 4°C. After washing as described, bound GT103 was detected with an anti-human IgG (γ-chain specific)-HRP conjugate (Chemicon Cat# AP504P). After washing as before, 1-Step ABTS (Thermo Fisher Cat# 37615) was added and color development was quantified by absorbance at 405 nm.

Calreticulin plasma membrane expression following GT103 treatment

H460 (human large cell lung cancer) and A549 (human lung adenocarcinoma) cells were grown in RPMI + fetal bovine serum (FBS) until 75% confluent. Cells were rinsed 3x with DPBS, then treated with 10% NHS and human GT103 or control antibody at 200 μg/ml for 2 hrs at 37°C. Doxorubicin (Sigma Cat# D1515) was used at 25 μM as a positive control. Cells were washed 3x with DPBS and detached with Versene. Plasma membrane protein was isolated using a plasma membrane protein extraction kit (101 Bio Cat# P503). Five μg of plasma membrane protein was loaded per lane in a Western blot. Blocking was done using 5% milk/PBST, and the blot was probed with an anti-calreticulin antibody (Thermo Fisher Cat# PA3-900, RRID:AB_325990) at a 1:1000 dilution for 2 hrs at room temperature in 5% milk/PBST. The membrane was probed with an anti-rabbit HRP secondary antibody at a 1:10000 dilution in 5%

milk/PBST for 1 hr at room temperature. The membrane was washed 4x with PBST following the primary and secondary antibody incubations. The blot was stripped and probed with a beta-actin antibody (R&D Cat# MAB8929) as a loading control. The experiment was repeated and whole cell lysate, rather than plasma membrane protein, was isolated after lysing cells with M-PER and probed with the anti-calreticulin antibody as described for the plasma membrane protein.

Immunofluorescence staining of frozen mouse tumors with anti-calreticulin antibody

Frozen CMT167 tumor sections were fixed with 4% paraformaldehyde for 15 minutes. Blocking was done in 5% goat serum/PBST for 1 hr at room temperature. The anti-calreticulin antibody (Thermo Fisher Cat# PA3-900) was used at a 1:75 dilution in 1% goat serum/PBST. An Alexa Fluor 488 goat anti-rabbit secondary antibody (Invitrogen Cat# A11008) was used at 10 μg/ml in 1% goat serum/PBST for 2 hrs at room temperature. Washes after primary and secondary antibody incubations, DNA staining, mounting, and imaging were performed as described above. The MFI of calreticulin was quantified using FIJI/ImageJ. The MFI of calreticulin was divided by the MFI of DNA stain for each spot to account for differences in the number of cells in each image.

C3b/iC3b deposition on human lung cancer cell lines following GT103 treatment

H460 or A549 human lung cancer cells were plated at concentration of 10^4 cells/well in a 96 well plate in RPMI (Thermo Fisher Cat# 11875-093) + 10% FBS. The following day, cells were washed 3x with DPBS and treated with antibody and normal human serum (NHS, Complement Technology, Inc.) as a source of complement. Human GT103 or a matched IgG control antibody were used at 200 μg/ml, while NHS was used at 10% of the final reaction volume. Cells were treated in 50% serum free RPMI and 50% 1x Veronal buffer (Lonza Cat#

12-624E). NHS was heat inactivated for 30 min at 56°C as a negative control, and in some experiments C1q depleted serum or Factor B depleted serum (Complement Technology, Inc. Cat#A300 and A335, respectively) were also used at 10% final dilution. The cells were treated for 24 hrs in a 37°C incubator. The following day, cells were detached with Versene solution (Thermo Fisher Cat# 15040-066), washed 3x with DPBS, and stained with allophycocyanin labeled anti-complement C3b/iC3b antibody (Biolegend Cat# 846105, RRID:AB_2632794) per the manufacturer's protocol. Samples were run on a FACSCanto analyzer and homogeneous populations of tumor cells were gated based on side and forward scatter, eliminating only debris.

C1q surface binding to a human lung cancer cell line following GT103 treatment

H460 cells were grown in culture, rinsed 3x in DPBS, and detached with Versene. $2.5x10^5$ cells were used in each condition, and each condition was run in duplicate. Cells were treated with 10% C4-depleted serum (Complement Technology, Inc. Cat#A308) in 50% RMPI and 50% Veronal buffer. C4-depleted serum was used to prevent complement mediated lysis induced by GT103 from occurring. Human GT103 and a matched IgG control antibody were used at 200 µg/ml, and cells were treated for 2 hrs at 37°C. In addition to GT103, a $F(ab')_2$ fragment of human GT103 was cloned and purified at the Duke Human Vaccine Institute and used in this experiment. The $F(ab')_2$ was used as additional control as it lacks CH2 in the Fc segment of the antibody to which C1q binds. Following treatment, cells were washed 3x with DPBS and stained with a C1q-FITC antibody (Thermo Fisher Cat# PA5-16601, RRID:AB_10984653) per the manufacturer's recommended protocol. Cells were washed 3x with DPBS and run on the FACSCanto analyzer, gating homogeneous populations of tumor cells based on side and forward scatter, eliminating debris.

Immunofluorescence staining of frozen mouse tumor with anti-C3b/iC3b/C3c antibody

CMT167 tumor sections were fixed in acetone for 5 minutes at room temperature and treated with 3% H_20_2/methanol for 10 minutes at room temperature to block endogenous peroxidases. Blocking was done in 5% goat serum/PBST for 1 hr at room temperature. An anti-C3b/iC3b/C3c antibody (Hycult Cat# HM1065, RRID:AB_10130996) was used at 1:25 dilution in 1% BSA/PBS. An Alexa Fluor 488 goat anti-rat secondary antibody (Invitrogen Cat# A11006) was used at 10 µg/ml in 1% goat serum/PBST for 2 hrs at room temperature. Washes after primary and secondary antibody incubations, DNA staining, mounting, and imaging were performed as described above.

Detection and quantification of C3d fragments in GT103 treated CMT167 tumors

CMT167 tumor lysates were made using M-PER (Thermo Fisher Cat# 78501) from the tumors of five GT103 treated mice and five control mice. 15 µg of protein from each tumor lysate was loaded per lane. The blot was blocked with 5% milk/PBST for 1 hr at room temperature and probed with an anti-C3d antibody (R&D Systems Cat# AF2655, RRID:AB_2066622) at 0.2 µg/ml in 5% milk/PBST for 2 hrs at room temperature. The blot was probed with a rabbit anti-goat HRP antibody (Santa Cruz Biotechnology, Inc. Cat# sc2768) at a 1:5000 dilution in 5% milk/PBST for 1 hr at room temperature. The blot was washed 4x with PBST following the primary and secondary antibody incubations. C3d and C3dg fluorescence was measured using Image Lab Software (BioRad).

Macrophage mediated ADCP following GT103 treatment

PBMCs were isolated from blood of a normal donor using Ficoll separation. As described in a previous publication (16), PBMCs at a concentration of $1x10^6$ cells/ml were plated in medium containing RMPI + 10% FBS, 8% NHS, 20 mM HEPES (Thermo Fisher Cat# 15630080), and 50 ng/ml hm-CSF (Cell Signaling Technology Cat# 8929). PBMCs were grown

in this medium for 5 days to allow the adherent cell population to differentiate into macrophages. Following this period, macrophages were detached with cold DPBS and labeled with CellTrace Violet (Thermo Fisher Cat# C34571). H460 cells were labeled with CFSE (Thermo Fisher Cat# C34554). Labeled macrophages were suspended in RPMI + 10% FBS at a concentration of $1x10^6$ cells/ml, while labeled H460 cells were suspended in the same medium at a concentration of $2x10^6$ cells/ml. A co-incubation step followed, where 50 µl of labeled tumor cells and 100 µl of labeled macrophages were added to the wells of a 96 well plate. Human GT103 or a matched IgG3 control antibody were added at 250 µg/ml. The co-incubation was done for 4 hrs in a 37°C incubator. Cells were detached with Versene and run on the FACSCanto analyzer. Initial gating was based on forward and side scatter to omit debris. From the resulting population of cells, macrophages were selected by gating for CellTrace Violet positive cells. From this population, cells doubly positive for CellTrace Violet-CFSE were selected. Each condition was run in duplicate, and phagocytosis was determined by calculating the percentage of doubly positive cells.

GT103-induced B cell Syk kinase phosphorylation

H460 lung cancer cells were plated at $2x10^4$ cells/well in a 96 well plate in RPMI + FBS media. The following day, cells were washed 3x with DPBS and treated with antibody and NHS. Human GT103 or a matched IgG3 control antibody were used at 200 µg/ml, while NHS was used at 10% of the final reaction volume. The cells were treated with antibody and serum for 1 hr in a 37°C incubator. PMBCs from a normal donor were isolated using a Ficoll gradient, and B cells were isolated using an isolation kit (Miltenyi Cat# 130-091-151). 8×10^4 B cells were added to each well of the 96 well plate containing tumor cells, and the cells were co-incubated for 24 hrs in a 37°C incubator. For western blot analysis of phosphorylated Syk, cells were detached

from the wells using Versene and protein was isolated using M-PER. 15 µg of protein from each co-incubation condition was loaded per lane. The blot was blocked with 5% milk/PBST for 1 hr at room temperature and probed with an anti-phospho-Syk antibody (Thermo Fisher Cat# MA5-14918, RRID:AB_10989513) at a 1:1000 dilution in 5% milk/PBST overnight at 4°C. The blot was probed with an anti-rabbit HRP secondary antibody (Thermo Fisher Cat# 65-6120) at 1:10000 dilution in 5% milk/PBST for 1 hr at room temperature. The blot was washed 4x with PBST following the primary and secondary antibody incubations. For flow cytometry experiments investigating phosphorylation of Syk, heat inactivated NHS and B cells not co-cultured with tumor cells were used as additional controls. Following co-incubation, cells were detached and stained with the anti-phospho-Syk antibody at 1:200 dilution using a Biolegend intracellular staining protocol. Cells were stained for 20 min at 4°C, washed, and stained with an anti-rabbit BV-421 secondary antibody (Biolegend Cat# 406410) at 1:50 dilution for 20 min at 4°C. Each condition was run in triplicate. B cells were gated based on size difference from tumor cells when samples were run on the FACSCanto analyzer.

Statistical Analyses

An unpaired, two-tailed Student's t-test was used for all analyses in which a p-value was derived.

Data Availability Statement

The raw sequence data reported in this paper have been deposited in the Sequence Read Archive database in National Library of Medicine, NCBI (https://www.ncbi.nlm.nih.gov). The raw data for single cell RNA sequencing are available under Bioproject accession number PRJNA936633. All other data generated in this study are available upon request from the corresponding author.

Results

GT103 has specificity for tumor tissue

We previously reported that GT103 causes CDC of tumor cells *in vitro* and postulated that its tumor specificity *in vivo* was due to an inhibitory effect on tumor growth while not affecting normal tissues (12). In this study, we further probed GT103 binding specificity to tumors vs. normal tissues by immunofluorescence. Using GT103 as a probe at concentrations of 5 and 50 μg/ml, we detected fluorescence in CMT167 tumor tissue (**Fig. 1A-B**),while at 50 μg/ml GT103 there was no detectable fluorescence in normal mouse lung or kidney (**Fig. 1C-D**). Minimal fluorescence was observed with anti-human secondary antibody alone.

To further investigate GT103 tumor specificity in human tissues, immunofluorescence was performed with a murine version of GT103 (mGT103) as primary antibody on TMA sections containing lung tumor tissues from 33 NSCLC patients and normal lung tissue. There were 19 females (10 anti-CFH autoantibody-positive and 9 autoantibody-negative) and 14 males (6 autoantibody-positive and 8 autoantibody-negative), with all stages of NSCLC represented. At 50 μg/ml GT103, variability in fluorescence was observed in tumor tissues (**Fig. 1E-G** show three examples) but essentially no detectable fluorescence was observed in normal human lung tissue (**Fig. 1H**).Quantified tumor GT103 fluorescence data for all 33 NSCLC patients is presented in Supplementary Data **Fig. S1**. No fluorescence was observed with anti-mouse secondary antibody alone.

In addition to exploring the binding of GT103 to human tumor or normal tissue, we were also interested in determining if GT103 could interact with fluid-phase CFH as it exists in the blood. To this end, we performed an ELISA designed to gauge the ability of purified soluble CFH to compete with an GT103 epitope-containing peptide for binding to GT103. After pre-

incubation of GT103 with up to a 12,800-fold molar excess of CFH for up to 24 h, no detectable effect on the binding of GT103 to immobilized epitope-containing peptide was observed (**Fig. 1I**).

GT103 increases calreticulin plasma membrane expression

We previously reported that GT103 causes cell death by CDC with release of the soluble complement activation products C3a and C5a (12). Complement activation, including the release of these pro-inflammatory cytokines, has been reported to increase the mobilization of DAMPs (17). Calreticulin, a canonical DAMP, is upregulated during cellular stress and, when translocated to the cell surface, promotes phagocytosis and antigen processing by immune cells (18,19). To determine whether GT103 treatment causes either upregulation of calreticulin or its translocation to the cell surface, H460 and A549 lung cancer cells were treated *in vitro* with GT103, control IgG, or doxorubicin, a known inducer of calreticulin translocation (19). Plasma membrane protein was isolated and subjected to western blotting with an anti-calreticulin antibody **(Fig. 2A)**. For H460 cells, the intensity of the calreticulin band normalized to beta-actin and expressed relative to a no antibody control was 1.92, 0.71, and 1.73 for the GT103, IgG3, and doxorubicin conditions, respectively. For A549 cells, the normalized calreticulin intensity was 2.23, 1.14, and 2.34 for the GT103, IgG3, and doxorubicin conditions, respectively. Thus, GT103 and doxorubicin were each found to increase plasma membrane calreticulin by approximately 2-fold over the IgG control in both cell lines. No change in calreticulin expression was detectible by western blot in whole cell lysates from GT103 treated cells. Tumors from mGT103- or control-treated mice and human NSCLC patients with or without the anti-CFH antibody were probed with anti-calreticulin antibody (**Fig. 2 B-I**). When CMT167 tumors were probed with a calreticulin antibody, mGT103-treated CMT167 tumors **(Fig. 2B-C)** exhibited

higher calreticulin immunofluorescence than control-treated CMT167 tumors **(Fig. 2D-E)**; green fluorescence values in the representative mouse tumor sections shown in **Fig. 2B-E** are quantitated in **Fig. 2H**.

We then wanted to determine if a similar pattern was seen in human lung cancer samples from patients with and without the anti-CFH autoantibody. By analogy of GT103 with the anti-CFH autoantibody from which it was derived, we hypothesized that tumors from CFH autoantibody-positive NSCLC patients would have higher cell surface calreticulin levels than tumors from CFH autoantibody-negative NSCLC patients. We probed a microarray containing 33 sections of human lung tumors and quantitated calreticulin immunofluorescence; examples of two such sections are shown in **Fig. 2F-G**. While there was variability among the 33 human samples overall, and overlap between the two populations, there was a significantly higher calreticulin immunofluorescence in the anti-CFH autoantibody-positive tumors than tumors from anti-CFH autoantibody-negative individuals (p=0.002) **(Fig. 2I)**.

GT103 causes deposition of C3 fragments on tumor cells and in tumor tissues via activation of the classical complement pathway

We have previously shown that GT103 causes complement activation *in vitro*; treatment of lung tumor cells with GT103 causes release of C3a, C5a, and deposition of C5b-9 (12). Here we determined whether GT103 causes an increase in C3b/iC3b deposition on tumor cells both *in vitro* and *in vivo.* While C3b deposition initiates the cascade that ultimately results in the formation of the membrane attack complex, three antigen-linked proteolytic degradation fragments of C3b – iC3b, C3dg, and C3d – bind to complement receptor 2 (CR2) via their common, exposed C3d moiety (20-24). Binding of these antigen-linked C3d-displaying fragments to CR2 receptors on B cells and follicular dendritic cells (DCs) results in activation of

B cells and augmentation of B cell affinity maturation by the follicular DCs displaying these antigens in germinal centers (25). GT103 caused a significant increase in C3b/iC3b deposition on the surface of A549 human lung cancer cells compared to a control IgG (p=0.001) (**Fig. 3A**). GT103 also caused a significant increase in C3b/iC3b deposition on the surface of human lung cancer H460 cells compared to control antibody (p=0.03) (**Fig. 3B**).

Sera depleted of Factor B and C1q were used to further investigate the pathway by which GT103 causes C3b/iC3b deposition on the H460 tumor cell surface: Factor B-depleted serum blocks alternative complement pathway activation, while C1q-depleted serum blocks classical pathway activation (26). Factor B-depleted serum combined with GT103 caused C3b/iC3b deposition similar to that caused by nondepleted NHS (p=0.25), while C1q-depleted serum with GT103 caused significantly lower C3b/iC3b on the H460 cell surface (p=0.01) (**Fig. 3B**). These results suggest that even though CFH regulates the alternative complement pathway, GT103 bound to CFH activates the classical complement pathway, in keeping with our previous report that CDC by GT103 primarily relies on the classical pathway (27).

The dependence of GT103-mediated C3b deposition and CDC on C1q suggested that C1q binding to tumor cells should be higher in the presence of GT103 than in its absence. To test this hypothesis, H460 cells were treated with GT103, control IgG, or a $F(ab')_2$ fragment of GT103 in the presence of C4-depleted serum (used to prevent complement mediated lysis induced by GT103 and preserve cell integrity). GT103 caused a significant increase in C1q binding to the cell surface compared to IgG control antibody (p=0.02) or the $F(ab')_2$ fragment (p=0.008) (**Fig. 3C**).

Following these *in vitro* results, we asked whether activated C3 products could be detected in CMT167 tumors in mice treated with mGT103. An immunofluorescent signal was

clearly detected in CMT167 tumors from mGT103 treated mice **(Fig. 3D-E)** with a primary antibody that detects C3b, iC3b, and C3c, while no detectable C3 fragments were detected in tumors from control treated mice **(Fig. 3F-G)**. No fluorescence was observed when secondary antibody was used alone. To differentiate C3b products that display the CR2 ligand C3d from those that do not, we assayed tumor lysates by western blot with a C3d-specific antibody that detects both C3dg and C3d (Supplementary Data **Fig. S2**). Mean levels of C3dg and C3d in CMT167 tumors of mGT103-treated mice were ~2-fold higher than those of control-treated mice (mean chemiluminescence intensity for C3dg: 113.8 vs. 69.7; C3d: 49.0 vs. 21.6). These experiments support previous observations that GT103 causes increased complement activation and suggest the intriguing possibility that GT103 treatment of tumor cells can cause activation of immune cells via the production of molecules that bind to the CR2 receptor.

GT103 promotes ADCP

The fact that GT103 induces CDC by the classical pathway implies that the antibody stably binds to its target on the cell surface, enabling Fc-C1q interaction. Therefore, we hypothesized that the Fc portion of GT103 bound to a tumor cell could also interact with the Fc receptor on a phagocytic cell, enabling ADCP of the tumor cell. We tested this hypothesis, with antibody-bound H460 tumor cells acting as the target and macrophages acting as the effector cell. GT103 caused significantly increased phagocytosis of H460 cells by macrophages compared to IgG control antibody ($p=0.002$) **(Fig. 3H)**.

GT103 activates B cells through Syk kinase phosphorylation

Among many downstream effects of complement activation, the interaction between complement C3 split products and CR2 on B cells links complement activation and humoral immunity through B cell activation (20). Co-culture experiments were performed to determine

whether GT103 mediated complement activation could have an activating effect on B cells. Phosphorylation of Syk, an intracellular tyrosine kinase that binds to the CD79a/CD79b signaling subunits of the B cell receptor (28,29), has been reported to be C3 fragment dependent and be crucial for B cell activation (20,30). When tumor cells were treated with GT103 and NHS as a source of complement, B cells were found to have significantly higher levels of phosphorylated Syk by western blot **(Fig. 4A)** and flow cytometry **(Fig. 4B)** compared to tumor cells treated with control antibody (p=0.04). Heat inactivating the NHS abolished the activation of Syk phosphorylation enabled by GT103 **(Fig. 4B)**.

B cell gene expression is activated in GT103-treated tumors

Because it appeared that B cells could be activated *in vitro* by complement split products generated by GT103, we investigated whether intratumoral B cells were activated by mGT103 *in vivo*. Tumors from mGT103 or control-treated CMT167-bearing mice were analyzed by scRNA-seq methods described elsewhere (15), here focusing on gene expression in B cells. Using principal component analysis, total B cell populations were grouped into 7 clusters (**Fig. 5A** and **Fig. 5B**). Notable upregulated genes relevant to B cells and their expression in mGT103-treated tumors relative to control-treated tumors are shown for the total B cell population in **Fig. 5C**, and for the CR2+ population (Cluster 1) in **Fig. 5D**, with lists of the top 25 upregulated and top 25 downregulated genes (including genes of unknown function), ordered by fold change, provided in Supplementary Data **Tables S1** and **S2**. GT103-upregulated genes were related to MHC class II antigen presentation (H2-DMa/ortholog of HLA-DMA), H2-Eb1/ortholog of HLA-DRB1, CD74 (31), and CD83 (32)); antibody production (IglC3/Ig lambda constant 3); germinal center function (Gpr183 (33) and Lmo2 (34)); and survival of mature B cells (Tnfrsf13C/BAFFR (35) and CD37 (36)). The upregulation of genes with B cell anergic functions (Ptpn6/Shp-1 (28) and

CD72 (37)) might possibly fill a negative feedback role in one or more subgroups of B cells.

GT103 activity *in vivo* is dependent on B cells

Saxena et al. (15) initially showed by bulk RNA sequencing of tumors that the top immunologically-related pathway upregulated by mGT103 in CMT167 mouse tumors was that of B cell receptor signaling. Here we showed by scRNA-seq that a number of functionally relevant genes are regulated by mGT103 in B cells. Given these results, we hypothesized B cells are required for mGT103 activity. To directly test this hypothesis, we performed an experiment in which B cells were depleted with an anti-CD20 antibody, CMT167 tumors were initiated, then mice were treated with mGT103 or subclass-matched control IgG2. Anti-CD20 antibody depleted intratumoral B cells efficiently (**Fig. 5E**). In the absence of B cells, mGT103 efficacy was abolished, demonstrating that B cells are essential for its antitumor activity (**Fig. 5F**).

Discussion

In a search for antibodies associated with a favorable outcome in NSCLC patients, we discovered an autoantibody to CFH (4,5). We have since found that GT103, a monoclonal antibody derived from this autoantibody, inhibits tumor growth and has many immune-stimulatory effects (12,15), but the mechanisms by which it exerts these effects have been unclear. Here we have focused on determining the effects of GT103 on immunity brought about by its activation of the complement system. The complement system is an essential part of innate immunity that eliminates pathogens and altered host cells, and when activated has wide-ranging immunological effects (38). In a cascade of proteolytic cleavages starting from the parent C3 molecule, complement "split" products are released and terminal MAC components are deposited in the membrane. Among the split products are the potent pro-inflammatory anaphylatoxins C3a and C5a and the biologically active degradation products of C3b.

Complement activation also acts as a bridge between the innate and adaptive immune systems since complement receptors are expressed on immune cells, including CR1 and CR2 on B cells and follicular DCs and CR3 on cells of the myeloid lineage in mice, with CR1 and CR2 expressed on additional cell types in humans (39).

A unified model for GT103 action, based on our current data and that of the Saxena et al report (15), is shown in **Fig. 6**. This mechanism draws links between complement activation mediated by GT103 and the modulation of adaptive immunity, all stemming from the tumor specificity of GT103. GT103 does not bind to native, soluble CFH, does not bind normal lung and kidney from mouse and human, yet does bind tumor tissue, which suggests this antibody will have an exceptional safety profile as a therapeutic without off-target effects. The possible binding of GT103 to kidney was tested because autoantibodies against CFH domains SCR 19-20 are associated with atypical hemolytic uremia syndrome (40). The epitope for GT103 is located in SCR 19, but is recognized only when the epitope is in a conformationally distinct form (12,13). The kidneys in GT103-treated mice (or humans expressing the GT103-related autoantibody) show no obvious damage, suggesting GT103 does not bind to CFH on normal kidney. The lack of binding of GT103 to kidney by immunofluorescence confirms this hypothesis. Although GT103 does not bind native CFH, chemically reducing CFH *in vitro* allows binding of GT103-related anti-CFH autoantibodies (13); it is possible that reduction of CFH within the reducing environment of a tumor exposes the epitope in a favorable conformation for antibody binding. Another possibility is that the altered glycoprotein composition of a tumor cell (41) causes CFH to bind to the membrane in a conformation that favors antibody binding. Regardless of how it is achieved, tumor specificity is important because it is the key to unleashing a local antitumor immune response without unwanted off-target

effects.

We previously found that GT103 kills tumor cells by inducing the classical pathway of CDC, and to a lesser extent, the alternative pathway (27). Using depleted sera lacking the capacity to carry out each pathway we showed that GT103 increased deposition of C3 fragments on tumor cells via the classical pathway; in addition, GT103, but not its $F(ab')_2$ fragment, increased binding of C1q to tumor cells. GT103-bound tumor cells also proved to be a target for macrophage-mediated ADCP, presumably through the recognition of immune complexes on the tumor cell surface by Fc receptors on macrophages.

Our data suggest that GT103-mediated CDC could potentially also lead to phagocytosis by a second mechanism: inducing translocation of surface exposed calreticulin to the plasma membrane during the process of immunogenic cell death. CDC of tumor cells has been described as a programmed or "necroptotic" cell death and not a simple osmotic lysis (42-44). Both apoptosis and necroptosis are forms of immunogenic cell death, one marker of which is the translocation of calreticulin to the plasma membrane (45,46). Plasma membrane calreticulin triggers engulfment of the dying cell by macrophages and DCs, followed by cross-presentation of cellular antigens (18,19,47), thus increasing the susceptibility of the cell to phagocytosis.

Our results also suggest that GT103-mediated CDC activates B cells *in vivo* by generating C3 split products in the tumors of GT103-treated tumor bearing mice, including increased C3d and C3dg. It is known that complement split products conjugated to cellular antigens lower the activation threshold of B cells by binding to the CR2 receptor via the C3d moiety (20). Furthermore, we showed a direct link between GT103-mediated complement activation and B cell activation through phosphorylated Syk *in vitro*. Previously, Saxena et al. (15) showed that in total tumor GT103 enhanced expression of genes in the B cell activation

pathway *in vivo*, and here we showed GT103 enhanced expression of B cell activation genes both in total intratumoral B cells and the intratumoral CR2+ B cell subset. Finally, we showed that B cells are required for inhibition of tumor growth by GT103 *in vivo*. Our results are reminiscent of those of Lu et al. (48), who demonstrated that chemotherapy in breast cancer patients and in mouse models of breast cancer generated a class of activated intratumoral Inducible T Cell Costimulator Ligand (ICOSL)+ B cells; generation of these cells was mediated by immunogenic cell death with exposure of the DAMP phosphatidylserine, and complement signaling through CR2. However, in our model, we did not see evidence of activation of the ICOSL gene.

GT103 is a novel antibody that holds tremendous promise in treating lung cancer and potentially other solid tumors that use a similar protective mechanism. By replicating the CFH autoantibodies found in early stage lung cancer patients with a favorable outcome, GT103 recognizes a unique tumor specific conformational target and has a novel mechanism of action. The antibody is being tested in a Phase 1b trial in patients with advanced stage NSCLC, and the data are currently being analyzed (https://clinicaltrials.gov/ct2/show/NCT04314089?term=gt103&draw=2&rank=1). Since this was a first-in-human trial, the study was designed to evaluate safety and tolerability, and determine a recommended Phase 2 dose. GT103 was found to be extraordinary safe, with only two potentially drug-related events (both self-limiting diarrhea), and was very well-tolerated. Even in this heavily pretreated population, preliminary data shows 24% had stable disease after treatment was initiated. There is now an extended cohort enrolling, as well as a Phase 2 combination trial with Pembrolizumab at a dose of 10 mg/kg set to begin in early 2023 (https://clinicaltrials.gov/ct2/show/NCT05617313?term=gt103&draw=2&rank=2), and future

studies are being planned in other cancer types.

The current report was intended to further highlight the specificity of GT103 and the multifarious mechanisms by which GT103-mediated complement activation initiates the development of an adaptive immune response. In future studies, clinical trial samples will enhance our efforts to discover potential biomarkers for GT103 efficacy, and also whether we can predict which patients will benefit the most from GT103 treatment.

Acknowledgments

This work was funded by the Department of Defense through Lung Cancer Research Program Translational Research Partnership Award No. W81XWH-19-1-0342 to E. F. Patz, Jr. and Y-W He; authors E. F. Patz, Jr., M. J. Campa, Y-W He, and R. Saxena were supported by this grant.

References

1. Schoenfeld AJ, Hellmann MD. Acquired Resistance to Immune Checkpoint Inhibitors. Cancer cell **2020**;37(4):443-55 doi 10.1016/j.ccell.2020.03.017.

2. Carmi Y, Engleman EG. Tumor-binding antibodies and tumor immunity. Oncotarget **2015**;6(34):35129-30 doi 10.18632/oncotarget.4889.

3. Carmi Y, Spitzer MH, Linde IL, Burt BM, Prestwood TR, Perlman N, *et al.* Allogeneic IgG combined with dendritic cell stimuli induce antitumour T-cell immunity. Nature **2015**;521(7550):99-104 doi 10.1038/nature14424.

4. Amornsiripanitch N, Hong S, Campa MJ, Frank MM, Gottlin EB, Patz EF, Jr. Complement factor H autoantibodies are associated with early stage NSCLC. Clin Cancer Res **2010**;16(12):3226-31 doi 10.1158/1078-0432.CCR-10-0321.

5. Gottlin EB, Campa MJ, Gandhi R, Bushey RT, Herndon 2nd JE, Patz Jr. EF. Prognostic significance of a complement factor H autoantibody in early stage NSCLC. Cancer Biomarkers **2022**;34(3):385-92.

6. Ajona D, Hsu YF, Corrales L, Montuenga LM, Pio R. Down-regulation of human complement factor H sensitizes non-small cell lung cancer cells to complement attack and reduces in vivo tumor growth. J Immunol **2007**;178(9):5991-8.

7. Horl S, Banki Z, Huber G, Ejaz A, Windisch D, Muellauer B, *et al.* Reduction of complement factor H binding to CLL cells improves the induction of rituximab-mediated complement-dependent cytotoxicity. Leukemia **2013**;27(11):2200-8 doi 10.1038/leu.2013.169.

8. Winkler MT, Bushey RT, Gottlin EB, Campa MJ, Guadalupe ES, Volkheimer AD, *et al.* Enhanced CDC of B cell chronic lymphocytic leukemia cells mediated by rituximab combined with a novel anti-complement factor H antibody. PLoS One **2017**;12(6):e0179841 doi 10.1371/journal.pone.0179841.

9. Junnikkala S, Jokiranta TS, Friese MA, Jarva H, Zipfel PF, Meri S. Exceptional resistance of human H2 glioblastoma cells to complement-mediated killing by expression and utilization of factor H and factor H-like protein 1. J Immunol **2000**;164(11):6075-81.

10. Varsano S, Rashkovsky L, Shapiro H, Ophir D, Mark-Bentankur T. Human lung cancer cell lines express cell membrane complement inhibitory proteins and are extremely resistant to complement-mediated lysis; a comparison with normal human respiratory epithelium in vitro, and an insight into mechanism(s) of resistance. Clinical and experimental immunology **1998**;113(2):173-82.

11. Wilczek E, Rzepko R, Nowis D, Legat M, Golab J, Glab M, *et al.* The possible role of factor H in colon cancer resistance to complement attack. Int J Cancer **2008**;122(9):2030-7.

12. Bushey RT, Moody MA, Nicely NL, Haynes BF, Alam SM, Keir ST, *et al.* A Therapeutic Antibody for Cancer, Derived from Single Human B Cells. Cell Rep **2016**;15(7):1505-13 doi 10.1016/j.celrep.2016.04.038.

13. Campa MJ, Gottlin EB, Bushey RT, Patz EF, Jr. Complement Factor H Antibodies from Lung Cancer Patients Induce Complement-Dependent Lysis of Tumor Cells, Suggesting a Novel Immunotherapeutic Strategy. Cancer Immunol Res **2015**;3(12):1325-32 doi 10.1158/2326-6066.CIR-15-0122.

14. Mao X, Zhou L, Tey SK, Ma APY, Yeung CLS, Ng TH, *et al.* Tumour extracellular vesicle-derived Complement Factor H promotes tumorigenesis and metastasis by inhibiting complement-dependent cytotoxicity of tumour cells. J Extracell Vesicles **2020**;10(1):e12031 doi 10.1002/jev2.12031.

15. Saxena R, Bushey R, Campa M, Gottlin E, Guo J, Patz E, *et al.* Creation of a Favorable Antitumor Microenvironment by the Anti-Complement Factor H Antibody GT103 (Preprint) **2022** https://doi.org/10.21203/rs.3.rs-2001920/v1.

16. Kamen L, Myneni S, Langsdorf C, Kho E, Ordonia B, Thakurta T, *et al.* A novel method for determining antibody-dependent cellular phagocytosis. Journal of immunological methods **2019**;468:55-60 doi 10.1016/j.jim.2019.03.001.

17. Kataoka H, Kono H, Patel Z, Kimura Y, Rock KL. Evaluation of the contribution of multiple DAMPs and DAMP receptors in cell death-induced sterile inflammatory responses. PLoS One **2014**;9(8):e104741 doi 10.1371/journal.pone.0104741.

18. Chao MP, Jaiswal S, Weissman-Tsukamoto R, Alizadeh AA, Gentles AJ, Volkmer J, *et al.* Calreticulin is the dominant pro-phagocytic signal on multiple human cancers and is counterbalanced by CD47. Sci Transl Med **2010**;2(63):63ra94 doi 10.1126/scitranslmed.3001375.

19. Obeid M, Tesniere A, Ghiringhelli F, Fimia GM, Apetoh L, Perfettini JL, *et al.* Calreticulin exposure dictates the immunogenicity of cancer cell death. Nat Med **2007**;13(1):54-61 doi 10.1038/nm1523.

20. Carroll MC, Isenman DE. Regulation of humoral immunity by complement. Immunity **2012**;37(2):199-207 doi 10.1016/j.immuni.2012.08.002.

21. Clemenza L, Isenman DE. Structure-guided identification of C3d residues essential for its binding to complement receptor 2 (CD21). J Immunol **2000**;165(7):3839-48 doi 10.4049/jimmunol.165.7.3839.

22. Kalli KR, Ahearn JM, Fearon DT. Interaction of iC3b with recombinant isotypic and chimeric forms of CR2. J Immunol **1991**;147(2):590-4.

23. Lyubchenko T, dal Porto J, Cambier JC, Holers VM. Coligation of the B cell receptor with complement receptor type 2 (CR2/CD21) using its natural ligand C3dg: activation

without engagement of an inhibitory signaling pathway. J Immunol **2005**;174(6):3264-72 doi 10.4049/jimmunol.174.6.3264.

24. Nagar B, Jones RG, Diefenbach RJ, Isenman DE, Rini JM. X-ray crystal structure of C3d: a C3 fragment and ligand for complement receptor 2. Science **1998**;280(5367):1277-81 doi 10.1126/science.280.5367.1277.

25. Merle NS, Noe R, Halbwachs-Mecarelli L, Fremeaux-Bacchi V, Roumenina LT. Complement System Part II: Role in Immunity. Front Immunol **2015**;6:257 doi 10.3389/fimmu.2015.00257.

26. Sarma JV, Ward PA. The complement system. Cell Tissue Res **2011**;343(1):227-35 doi 10.1007/s00441-010-1034-0.

27. Bushey RT, Gottlin EB, Campa MJ, Patz EF, Jr. Complement factor H protects tumor cell-derived exosomes from complement-dependent lysis and phagocytosis. PLoS One **2021**;16(6):e0252577 doi 10.1371/journal.pone.0252577.

28. Franks SE, Cambier JC. Putting on the Brakes: Regulatory Kinases and Phosphatases Maintaining B Cell Anergy. Frontiers in immunology **2018**;9:665 doi 10.3389/fimmu.2018.00665.

29. Heizmann B, Reth M, Infantino S. Syk is a dual-specificity kinase that self-regulates the signal output from the B-cell antigen receptor. Proc Natl Acad Sci U S A **2010**;107(43):18563-8 doi 10.1073/pnas.1009048107.

30. Ackermann JA, Nys J, Schweighoffer E, McCleary S, Smithers N, Tybulewicz VL. Syk tyrosine kinase is critical for B cell antibody responses and memory B cell survival. J Immunol **2015**;194(10):4650-6 doi 10.4049/jimmunol.1500461.

31. Schroder B. The multifaceted roles of the invariant chain CD74--More than just a chaperone. Biochim Biophys Acta **2016**;1863(6 Pt A):1269-81 doi 10.1016/j.bbamcr.2016.03.026.

32. Kuwano Y, Prazma CM, Yazawa N, Watanabe R, Ishiura N, Kumanogoh A*, et al.* CD83 influences cell-surface MHC class II expression on B cells and other antigen-presenting cells. Int Immunol **2007**;19(8):977-92 doi 10.1093/intimm/dxm067.

33. Choi C, Finlay DK. Diverse Immunoregulatory Roles of Oxysterols-The Oxidized Cholesterol Metabolites. Metabolites **2020**;10(10) doi 10.3390/metabo10100384.

34. Natkunam Y, Zhao S, Mason DY, Chen J, Taidi B, Jones M*, et al.* The oncoprotein LMO2 is expressed in normal germinal-center B cells and in human B-cell lymphomas. Blood **2007**;109(4):1636-42 doi 10.1182/blood-2006-08-039024.

35. Mackay F, Schneider P. Cracking the BAFF code. Nat Rev Immunol **2009**;9(7):491-502 doi 10.1038/nri2572.

36. van Spriel AB, de Keijzer S, van der Schaaf A, Gartlan KH, Sofi M, Light A, *et al.* The tetraspanin CD37 orchestrates the alpha(4)beta(1) integrin-Akt signaling axis and supports long-lived plasma cell survival. Sci Signal **2012**;5(250):ra82 doi 10.1126/scisignal.2003113.

37. Parnes JR, Pan C. CD72, a negative regulator of B-cell responsiveness. Immunol Rev **2000**;176:75-85 doi 10.1034/j.1600-065x.2000.00608.x.

38. Dunkelberger JR, Song WC. Complement and its role in innate and adaptive immune responses. Cell Res **2010**;20(1):34-50 doi 10.1038/cr.2009.139.

39. Carroll MC. Complement and humoral immunity. Vaccine **2008**;26 Suppl 8:I28-33 doi 10.1016/j.vaccine.2008.11.022.

40. Blanc C, Roumenina LT, Ashraf Y, Hyvarinen S, Sethi SK, Ranchin B, *et al.* Overall neutralization of complement factor H by autoantibodies in the acute phase of the autoimmune form of atypical hemolytic uremic syndrome. J Immunol **2012**;189(7):3528-37 doi 10.4049/jimmunol.1200679.

41. Christiansen MN, Chik J, Lee L, Anugraham M, Abrahams JL, Packer NH. Cell surface protein glycosylation in cancer. Proteomics **2014**;14(4-5):525-46 doi 10.1002/pmic.201300387.

42. Fishelson Z, Kirschfink M. Complement C5b-9 and Cancer: Mechanisms of Cell Damage, Cancer Counteractions, and Approaches for Intervention. Frontiers in immunology **2019**;10:752 doi 10.3389/fimmu.2019.00752.

43. Lusthaus M, Mazkereth N, Donin N, Fishelson Z. Receptor-Interacting Protein Kinases 1 and 3, and Mixed Lineage Kinase Domain-Like Protein Are Activated by Sublytic Complement and Participate in Complement-Dependent Cytotoxicity. Frontiers in immunology **2018**;9:306 doi 10.3389/fimmu.2018.00306.

44. Ziporen L, Donin N, Shmushkovich T, Gross A, Fishelson Z. Programmed necrotic cell death induced by complement involves a Bid-dependent pathway. J Immunol **2009**;182(1):515-21.

45. Vandenabeele P, Vandecasteele K, Bachert C, Krysko O, Krysko DV. Immunogenic Apoptotic Cell Death and Anticancer Immunity. Adv Exp Med Biol **2016**;930:133-49 doi 10.1007/978-3-319-39406-0_6.

46. Sprooten J, De Wijngaert P, Vanmeerbeerk I, Martin S, Vangheluwe P, Schlenner S, *et al.* Necroptosis in Immuno-Oncology and Cancer Immunotherapy. Cells **2020**;9(8) doi 10.3390/cells9081823.

47. Zitvogel L, Kepp O, Senovilla L, Menger L, Chaput N, Kroemer G. Immunogenic tumor cell death for optimal anticancer therapy: the calreticulin exposure pathway. Clin Cancer Res **2010**;16(12):3100-4 doi 10.1158/1078-0432.CCR-09-2891.

48. Lu Y, Zhao Q, Liao JY, Song E, Xia Q, Pan J, *et al.* Complement Signals Determine Opposite Effects of B Cells in Chemotherapy-Induced Immunity. Cell **2020**;180(6):1081-97 e24 doi 10.1016/j.cell.2020.02.015.

Figure Legends

Figure 1. Tumor specificity of GT103 in NSCLC. (A-H) Immunofluorescence of tumor and normal tissues probed with GT103. To avoid unwanted cross-reaction of secondary antibodies with IgG in tissues, mouse tissues were probed with human GT103 and human tissues with mGT103. **(A-D)** GT103 binding to mouse tissue. GT103 binding to CMT167 mouse cell line tumors was observed at **(A)** 5 μg/ml or **(B)** 50 μg/ml GT103, while no binding was observed in **(C)** normal mouse lung or **(D)** normal mouse kidney, both at 50 μg/ml GT103. Representative images are shown; multiple tumor, lung, and kidney samples were probed with GT103 and identical results were observed. **(E-H)** mGT103 binding to human tissue. Thirty-three human lung tumor spots on a TMA were probed with mGT103 at 50 μg/ml and three representative images showing variability in staining are shown **(E-G)**. No fluorescence was detected in multiple normal human lung tissue samples probed with mGT103 at the same concentration; a representative image is shown in **(H)**. No fluorescence was observed for any samples with secondary antibody in the absence of GT103. **(I)** ELISA data showing the inability of soluble CFH to interfere with the interaction of GT103 with immobilized epitope peptide.

Figure 2. Plasma membrane expression of calreticulin increases following GT103 treatment. (A) Anti-calreticulin western blots of plasma membrane and total lysates of tumor cells treated *in vitro* with GT103 or control. H460 and A549 cells were treated with GT103 or control IgG in the presence of NHS, or with doxorubicin as a positive control. Plasma membranes or whole cell lysates were prepared and subjected to western blot analysis. Top panel: Plasma membrane blot probed with anti-calreticulin antibody; Middle panel: Same blot stripped and probed with anti-beta-actin antibody (loading control); Bottom panel: Whole lysate blot probed with anti-calreticulin antibody. **(B-G)** Immunofluorescence for calreticulin in tumors

of GT103- or control treated mice or tumors of anti-CFH autoantibody-positive and -negative NSCLC patients. CMT167 tumor sections from GT103-treated **(B,C)** or control-treated **(D,E)** mice were probed with anti-calreticulin and secondary antibodies. Human lung tumor sections from anti-CFH autoantibody-negative or -positive patients were similarly stained; two such sections are shown in panels **(F,G)**. Human lung tumor samples on a TMA were also stained for calreticulin, images of two fields were captured for each of the 33 spots stained with calreticulin antibody, and the mean normalized MFI of calreticulin was determined. Panel **(H)** shows quantitation of calreticulin in the four mouse tumor samples (mean of two images/sample with SD). Variability in fluorescence between the human samples is represented in panel **(I)**. There was a significant difference in calreticulin MFI between anti-CFH autoantibody-positive and -negative samples (mean MFI of positive group = 1.32; mean MFI of negative group = 0.92; p=0.002). No background fluorescence was observed for mouse or human samples with secondary antibody alone.

Figure 3. GT103 causes deposition of complement split products on tumor cells *in vitro* and *in vivo* via the classical complement pathway. (A-B) C3b/iC3b deposition on tumor cells. **(A)** A549 and **(B)** H460 human lung cancer cells were treated *in vitro* with GT103 or IgG in the presence of NHS or heat-inactivated (HI) NHS. In **(B)**, cells were also incubated with antibodies in the presence of C1q-depleted or Factor B-depleted NHS. C3b/iC3b binding to cells was measured by flow cytometry. Each condition was run in triplicate, and the data are shown as mean C3b/iC3b fluorescence ± SD. **(C)** C1q deposition on H460 lung cancer cells. Cells were treated with GT103, the $F(ab')_2$ of GT103, or subtype-matched IgG in C4-depleted NHS (used to supply complement but not allow cell lysis). C1q binding was measured by flow cytometry. Each condition was run in triplicate, and the data are shown as C1q fluorescence ± SD. **(D-G)**

CMT167 tumors from mouse studies were analyzed for C3 fragments (C3b/iC3b/C3c) by immunofluorescence. GT103 treated CMT167 tumors **(D-E)** were compared to control treated CMT167 tumors **(F-G)**. For (**A-C**), flow cytometry histograms illustrating key comparisons are shown in Supplementary Data **Fig. S3**. **(H)** Macrophage-mediated ADCP of H460 lung cancer cells *in vitro*. Macrophages and tumor cells were labeled with different fluorophores and either no antibody, human GT103, or matched IgG control antibody were added at 250 μg/ml. In order to measure ADCP (as opposed to complement dependent cellular cytotoxicity), no serum was present. After coincubation of macrophages and tumor cells, doubly positive cells were isolated by flow cytometry. The flow cytometry gating strategy for this experiment and representative results are shown in Supplementary Data **Fig. S4**. Each condition was performed in triplicate and means $\pm$ SD are plotted.

Figure 4. GT103 induces phosphorylation of Syk kinase in B cells co-cultured with tumor cells. H460 lung cancer cells were treated with GT103 or IgG in the presence of normal human serum (NHS) and then co-cultured with B cells for 24 hrs. **(A)** Lysates of the cell mixtures were probed with an antibody against phosphorylated Syk by immunoblot. **(B)** The same experimental setup was performed, with the addition of controls in which B cells were incubated in the absence of tumor cells, or heat inactivated (HI) NHS was substituted for NHS, and B cells were permeabilized, gated and stained for phosphorylated Syk by flow cytometry. The flow cytometry gating strategy for this experiment and a representative result are shown in Supplementary Data **Fig. S5**. Each condition was run in triplicate, and phospho-Syk fluorescence is represented as mean ± SD.

Figure 5. mGT103 activates B cell gene expression in CMT167 tumors and tumor growth inhibition is dependent on intratumoral B cells. (A-D) Analysis of intratumoral B cell gene

expression. Six- to eight-week old C57BL/6 mice were injected with CMT167 tumor cells and randomly divided; one group was treated with mGT103 and the other with mIgG2 as described in Materials and Methods. Tumors from 3 treated mice in each group were dissociated, and the cells pooled and analyzed by scRNA-seq. Clusters identified as B cells were subclustered using the Seurat FindClusters function as previously described (15). **(A)** A t-distributed stochastic neighbor embedding (t-SNE) plot showing distribution of B cells per cluster in mGT103- and control-treated groups. **(B)** Stacked bar plot showing the subcluster composition of B cells per sample. Relative expression (log fold change) of selected GT103-upregulated genes in **(C)** the total B cell population and **(D)** the CR2+ B cell population are shown. **(E-F)** Analysis of dependence of GT103 activity on B cells. Ten six- to eight-week old C57BL/6 mice were injected with anti-CD20 three days prior to tumor inoculation (Day -8) to deplete B cells. On Day -5, 10 B cell-depleted and 10 nondepleted C57BL/6 mice were inoculated s.c. with CMT167 cells. On Day 0, when tumors were palpable, mice in each group were dosed three times a week with control IgG2 or GT103 i.p. as described in Materials and Methods. After sacrifice, tumors were analyzed for B cell depletion by flow cytometry. **(E)** Percent of CD19+ B cells as a percentage of total CD45+ tumor infiltrating leukocytes isolated from the CMT167 dissected tumors, as analyzed by flow cytometry. **(F)** Tumor volume was plotted as mean ± SEM for n=3-5 for each treatment group.

Figure 6. Proposed unified mechanism for GT103 action. GT103 binds to an epitope in tumor cell-associated CFH that is only revealed in the tumor environment (indicated by red dot). Binding of GT103 on the tumor cell surface allows C1q binding, triggering CDC by the classical pathway. Membrane attack complexes (MAC) accumulate on the cell surface, leading to cell death and translocation of calreticulin (CRT) from the endoplasmic reticulum (ER) to the plasma

membrane (PM). Phagocytic cells recognize CRT via specific receptors and the bound antibody via Fc gamma receptors, leading to phagocytosis and antigen presentation to T cells. During CDC, key immune modulatory molecules are released. The C3d moiety of several C3b split products, bound to antigen, binds to CR2 on B cells; the CR2-C3d complex then presents the antigen to a cognate B cell receptor, whereupon the B cell becomes activated, promoting further tumor cell killing. C3d is also proposed to bind to two receptors on intratumoral T regulatory cells (itTREGS) decreasing expression of the Id2 transcription factor, leading to deletion of these immunosuppressive cells. During CDC, C3a and C5a are also released and bind to their receptors on CD4+ and CD8+ T cells, activating them. See Saxena et al. (15) for evidence supporting the T cell segments of this proposed mechanism.

Figure 1

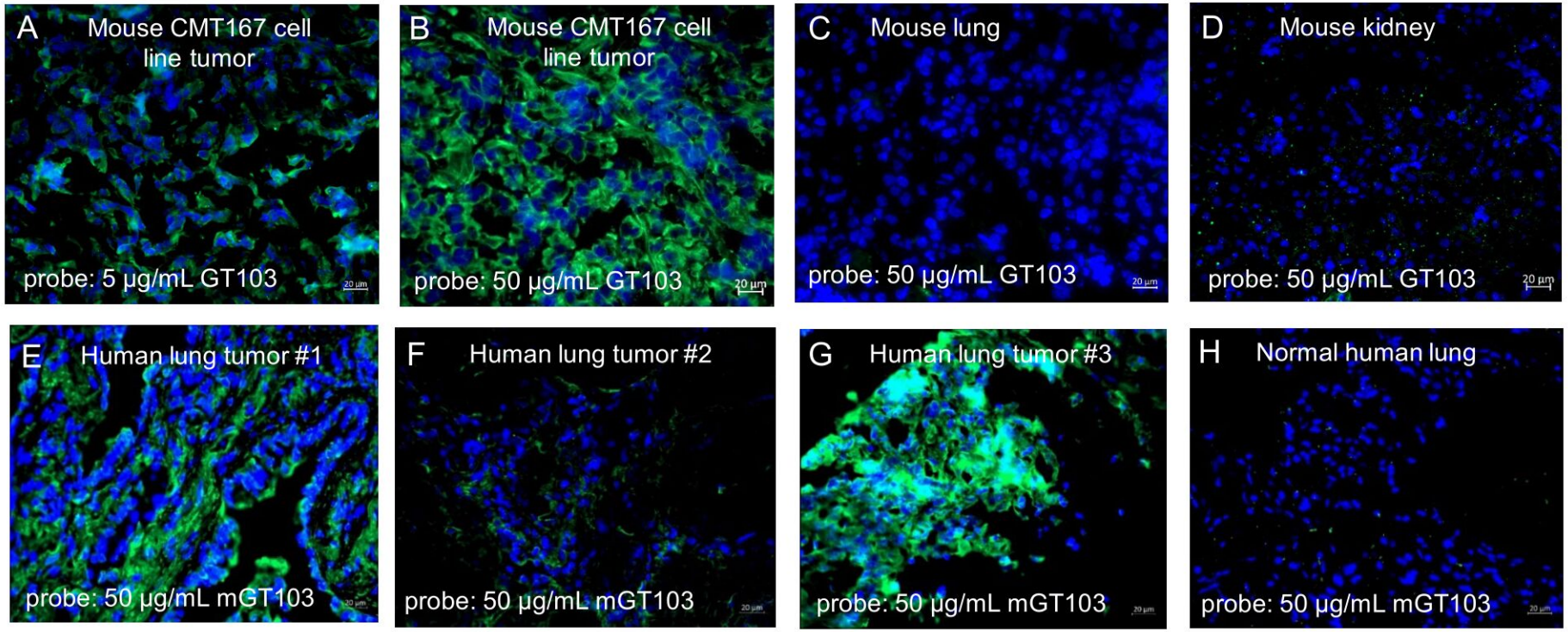

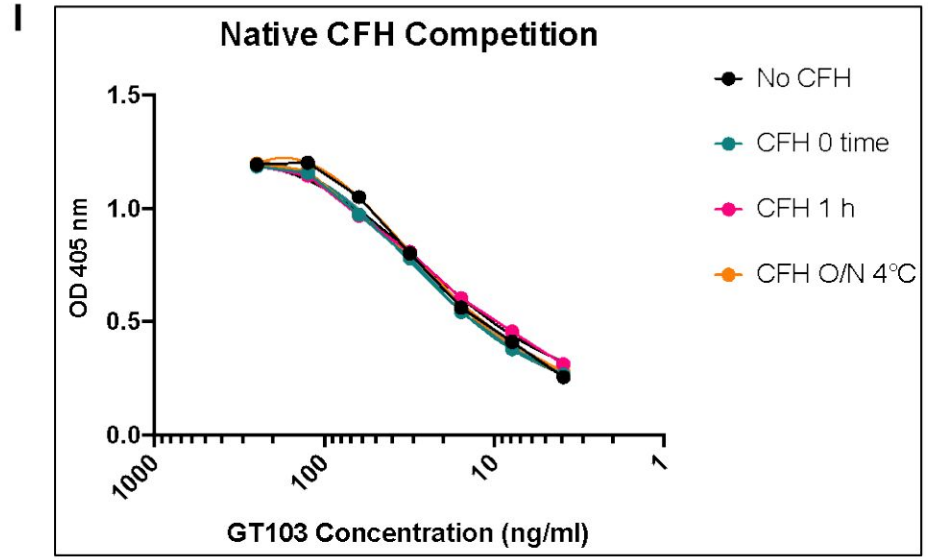

Figure 2

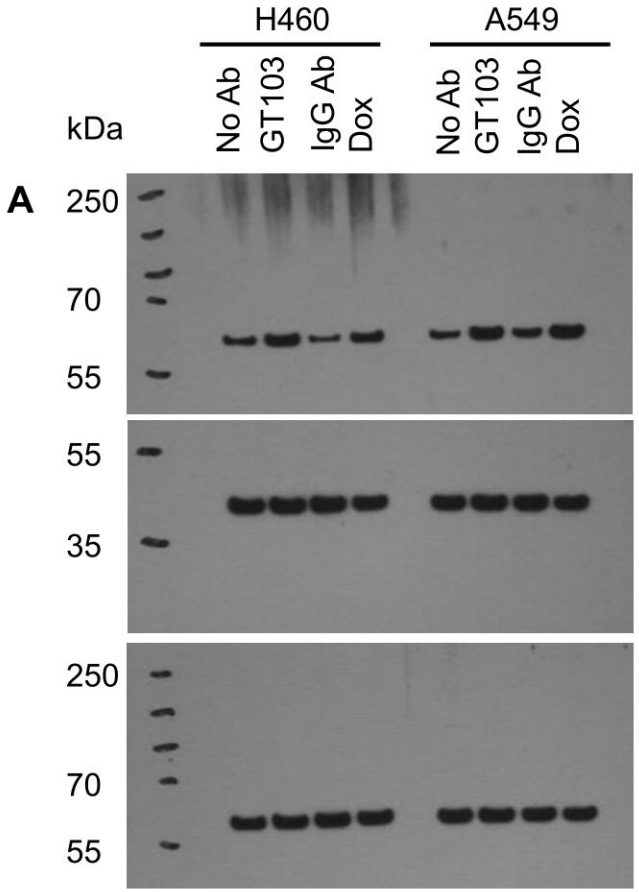

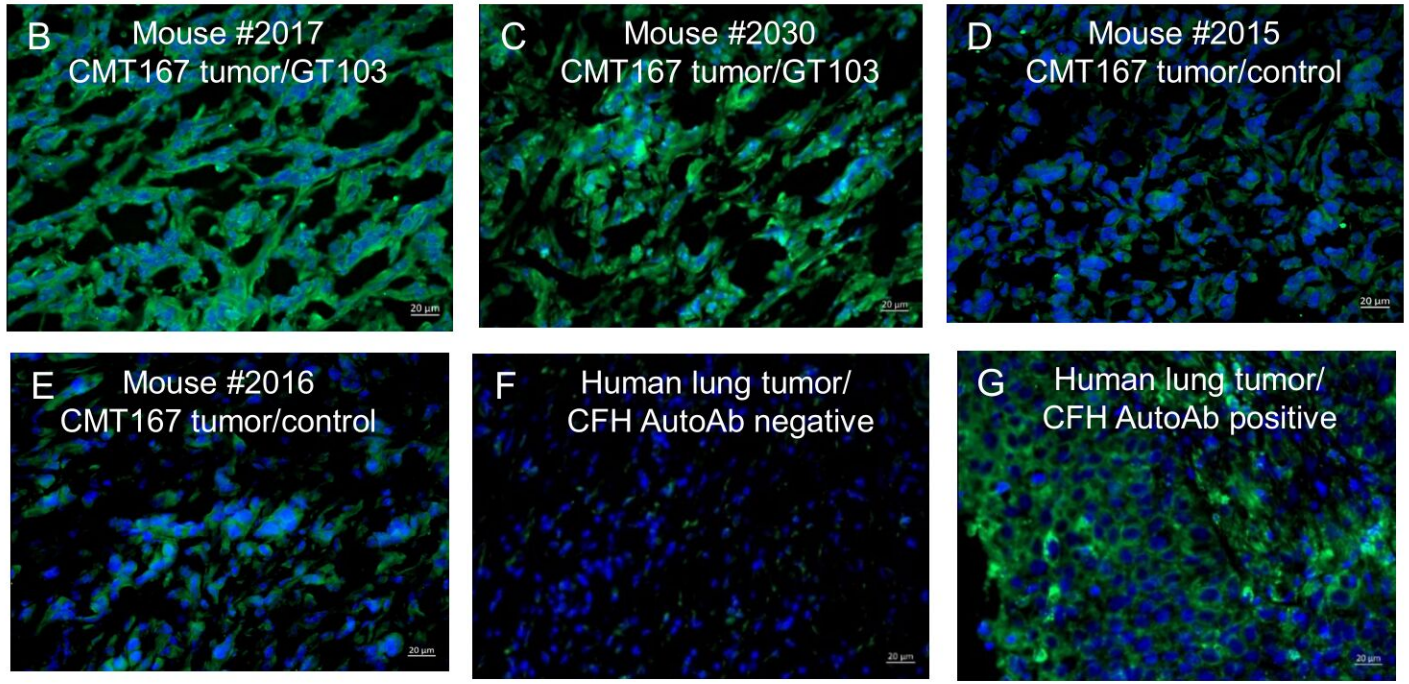

B-G tumor sections probed with anti-calreticulin antibody

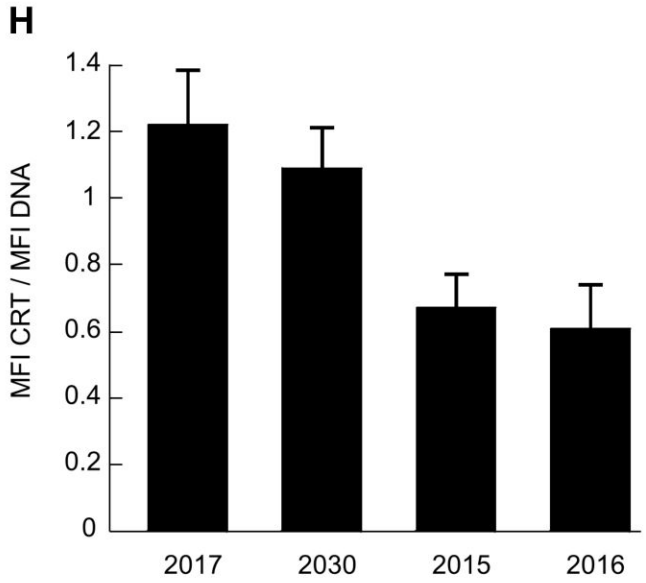

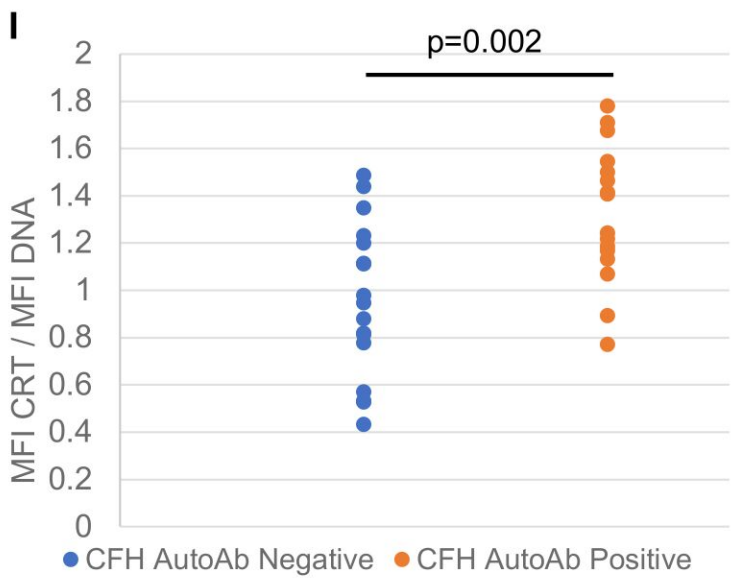

Figure 3

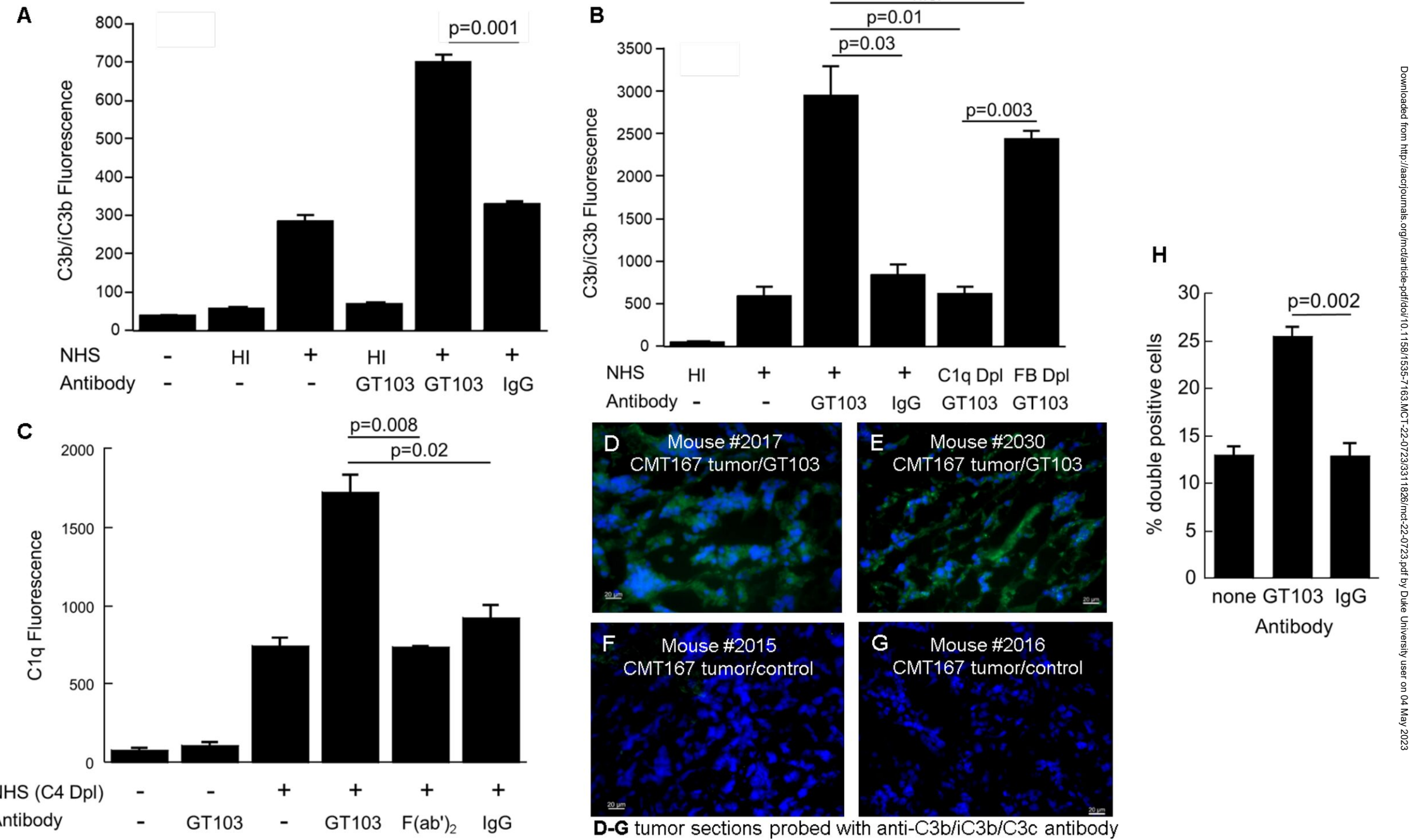

D-G tumor sections probed with anti-C3b/iC3b/C3c antibody

Figure 4

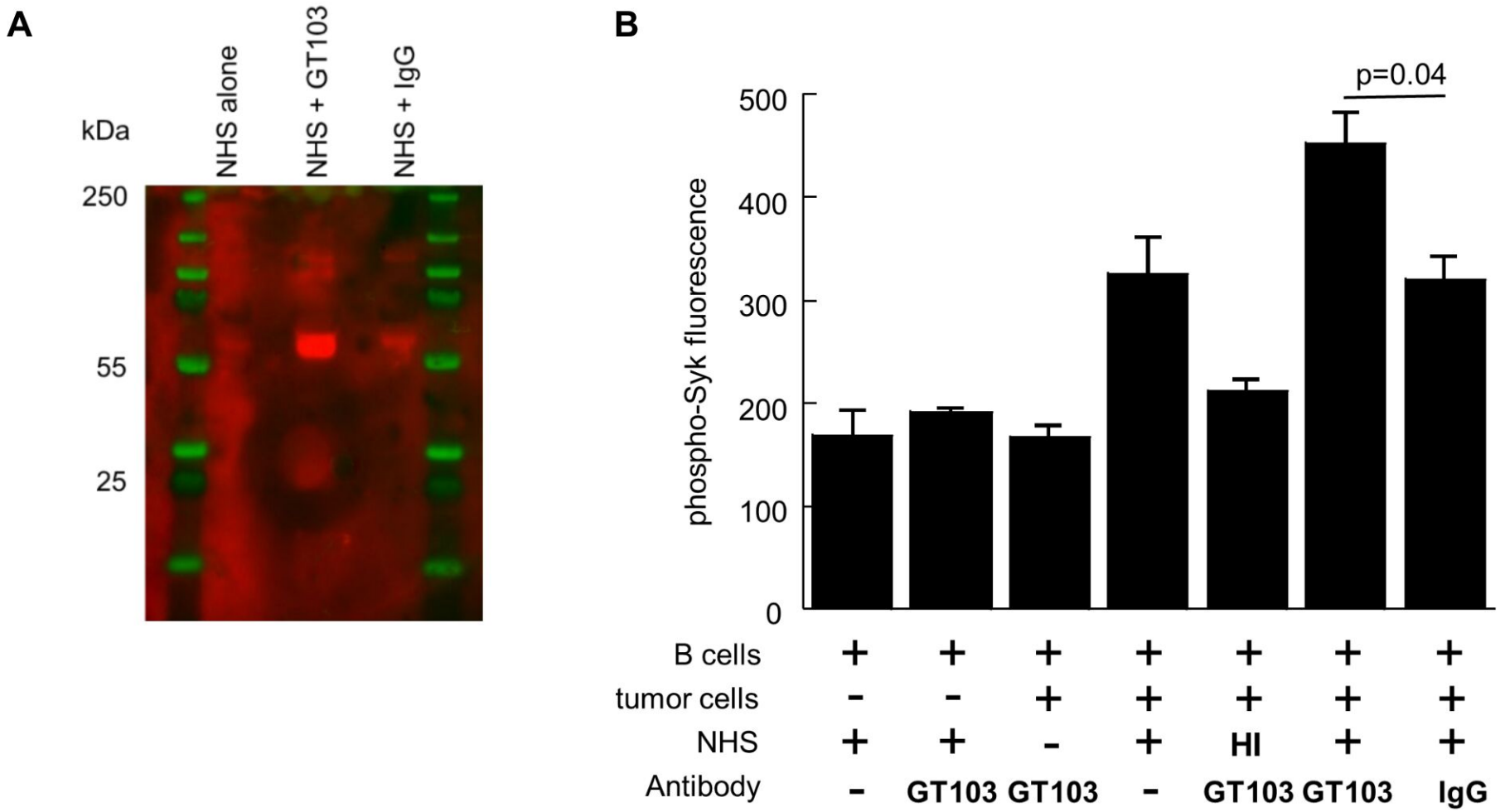

Figure 5

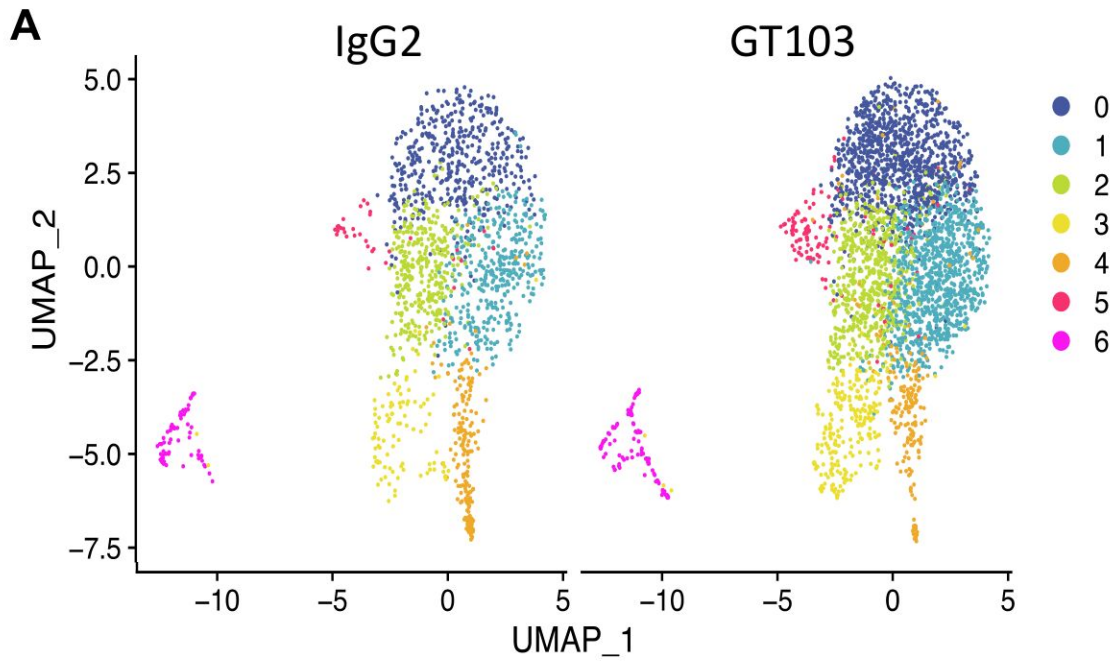

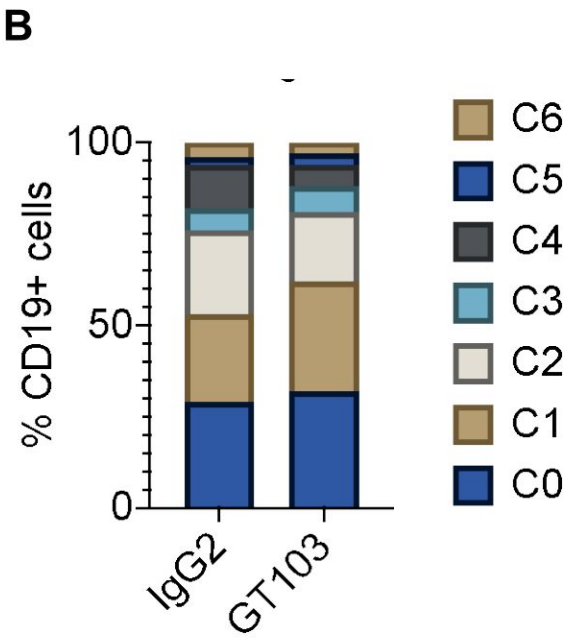

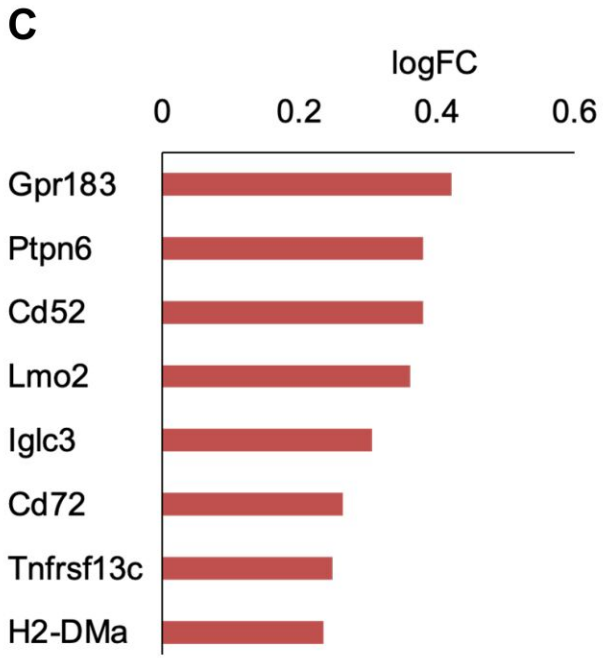

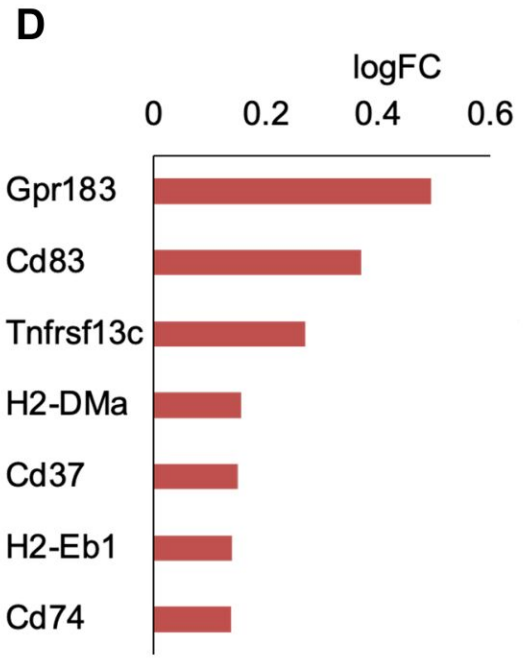

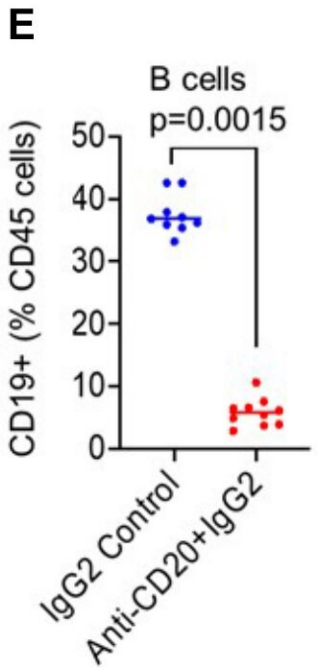

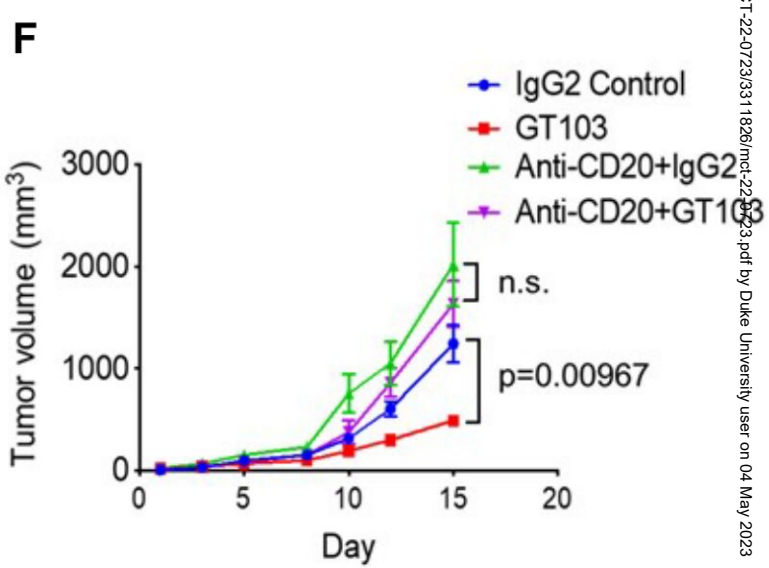

Figure 6